Journal of Electronics and Information Science(2017) 2: 62-71
Clausius Scientific Press, Canada

A Simple Method for Predicting System Flow Rates of Telecom Rack

Lian-Tuu Yeh, Ph D & PE

ASME Fellow
Dallas, TX
Email: jjyeh2@aol.com

Keywords: Predicting system, Flow Rates, Telecom Rack.

Abstract: A simple and effective method based on the fluid network resistance model is developed to accurately predict system flow rate. This is especially useful for determining the effects of various parameters of the telecommunication equipment configuration on the system flow rate. Though the method presented can directly be employed to calculate the system flow as well as the flow rates of individual printed circuit boards (PCBs), however the present study is focusing at the analysis to generate a family of curves serving as the design guidelines which can quickly and accurately predict the effect of the changes of individual parameters on the system flow rate.

1. Introduction

The sketch of a typical telecommunication system is given in Figure 1. As illustrated in the figure, the key elements of the system include the card cage which hosts the printed circuit boards, air filter, electric magnetic insulation (EMI) plates which prevent electric magnetic waves from leaking into the ambient, and the fan trays in the forced air cooling systems. In addition, the system also includes an air inlet section and an outlet section.

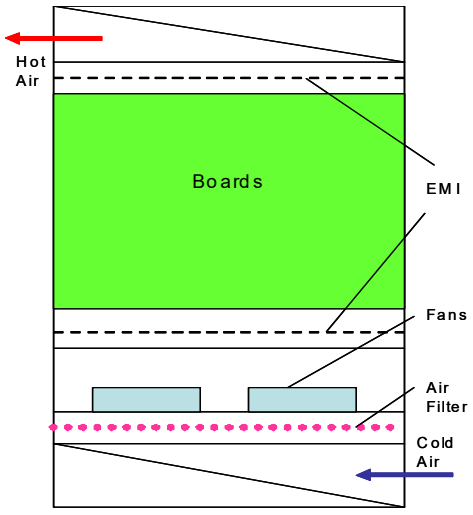

Figure 1 Side View of a Typical Telecommunication System

The system level thermal analysis is first performed to calculate system flow rate and the flow rate to individual boards which is often also referred to as the slot flow rate. The computed slot flow rate will then be applied to the individual boards for the board level thermal analysis which is to determine the temperature of the components on the individual boards.

Since the detailed information of individual boards is generally not available in the early phase of design cycle, one must assume some values of pressure drop for the boards. This assumed value

can be obtained from the existing similar boards or just from the preliminary board layout. The assumption of this value is not very critical for the purpose of the system level flow analysis. The reason is that the pressure drop over the board is typically less than 1/3 of the total system pressure drop. Therefore, the effects of the errors in the initial estimate on the system flow rate will be limited. In addition, the more accurate estimated pressure drop over the board will be available once the detailed board is developed.

A CFD (computational fluid dynamic) analysis tool is generally employed for the system thermal and flow analyses. However, a much simple approach or even with hand calculations can be made to predict the system flow rate by using the flow resistance network model which will be described in the follow section.

2. Analysis

The flow network method will be employed in the analysis. Figure 2 shows the simple sketch of a representative telecommunication shelf and its flow resistance over the system. The individual flow resistance is as follows:

R1 = entrance
R2 = inlet section
R3 = 90 degree turn
R4 =air filter
R5 = card cage, including 2 EMI plates
R6 = 90 degree turn
R7 = exit section
R8 = exit

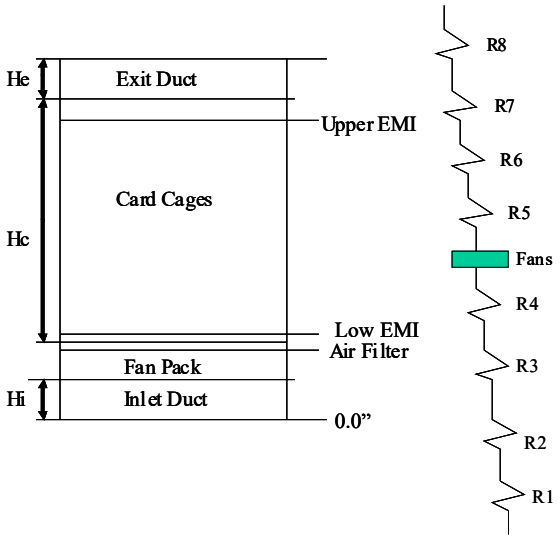

Figure 2 Sketch of System and Its Flow Network Resistance

The flow resistance can be expressed by the following equation

$$\Delta P = K\,(0.5\,\rho\,V^2) = R\,Q^2 \qquad (1)$$

Where K is the loss coefficient, R (=0.5 K ρ/A^2) is the flow resistance, Q (= AV) is the volumetric flow rate and A is the cross section area and V is the average velocity across this cross section area.

Basically, the system flow rate is determined by the fan operation point which is defined as the intersection point of the fan performance curve and the system pressure drop curve. The system pressure drop is the sum of the pressure drop over the inlet, turns, air filter, EMI plates, boards and

exit.

Although the present method can be used to compute the system flow rate, this study is mainly to examine the effects of various parameters of the configuration on the system flow rate. For purpose of practical applications, a family of curves is developed serving as the design guidelines which can quickly predict the effect of the changes of individual parameters on the system flow rate.

-- Effect of System Height

Figure 3 illustrates the system configuration under consideration. Hi is the height of the inlet and exit. It should be noted that the height of the inlet can be different from that of the exit. For simplicity, both the inlet and exit assume to have the same height. Additional assumptions are as follows:

1) All flow resistance from R1 through R8 of the baseline configuration are known
2) Except the height, all other dimensions of the system remain unchanged
3) Flow resistance of other sections or parts of the system are unchanged

From Equation (1), one obtains the following relationship for the inlet and the exit

$$R \quad \alpha \quad (1/H^2) \tag{2}$$

Where H is the height of the inlet and the exit sections

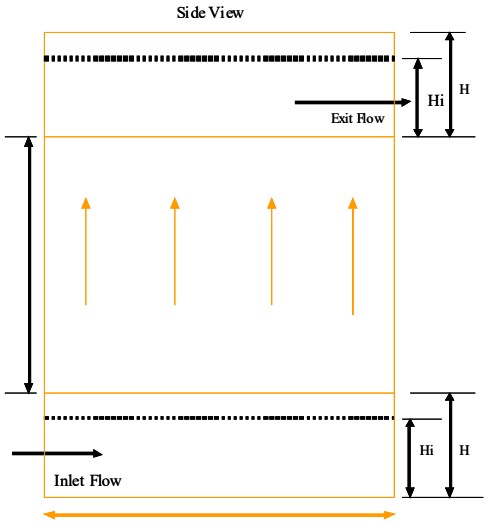

Figure 3 Sketch of System with Various Inlet/Exit Heights

Based on the above assumptions,

$$R / (R)bl = (Hi / H)^2 \tag{3}$$

Where (R)bl and Hi are the flow resistance and inlet/exit height of the baseline configuration, respectively. It should be noted that the inlet height can be different from the exit height.

Equation (3) states that increasing the inlet height (H > Hi) will decrease the inlet flow resistance. The next step is to calculate the new total system flow resistance, Rt based on the calculated flow resistance for the inlet/exit. Once the new system flow resistance is known, the system new flow rate can readily be determined by the following equation

$$Q / (Q)bl \quad = [(Rt)bl / Rt]^{0.5} \tag{4}$$

The following example is to show how to compute the new system total flow resistance and the flow rate

Example 1 : For H/Hi = 1.5,

From Equation (3), one obtains

$$R18 = 0.4444 \ (R18)bl \tag{5}$$

Assuming (R18)bl [=(R1+ R8)bl] = 0.1 (Rt)bl for the baseline configuration, then the new total system flow resistance for H/Hi = 1.5 is computed as follows

$$Rt = 0.1 \times R18 + 0.9\,(Rt) = 0.94444\,(Rt)bl \quad (6)$$

And the new volumetric flow rate with H/Hi = 1.5 is

$$Q / (Q)bl = [\,(Rt)bl / Rt]^{0.5} = [\,0.94444]^{0.5} = 1.029 \quad (7)$$

Equation (7) implies that the inlet/exit height increases by 50%, the system flow rate increases by about 3% for (R18)bl = 0.1 (Rt)bl if other parameters of the system remain unchanged.

Following the above procedure, the family of the curves is developed for the modified system as shown in Figures 4 and 5 for the new flow resistance and the new flow rate, respectively.

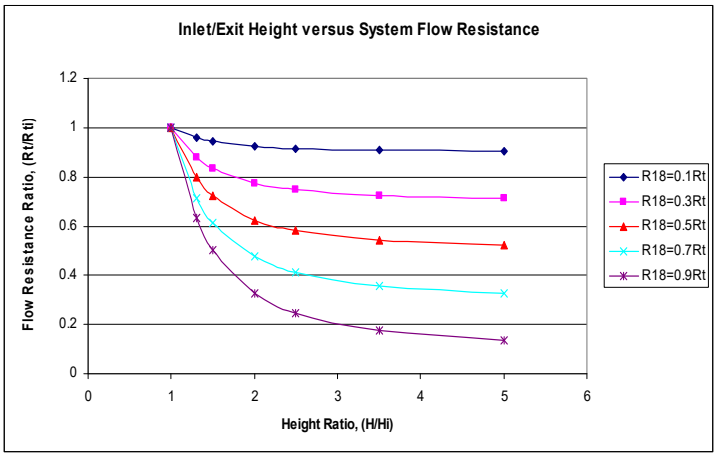

Figure 4 Inlet/Exit Height versus System Flow Resistance

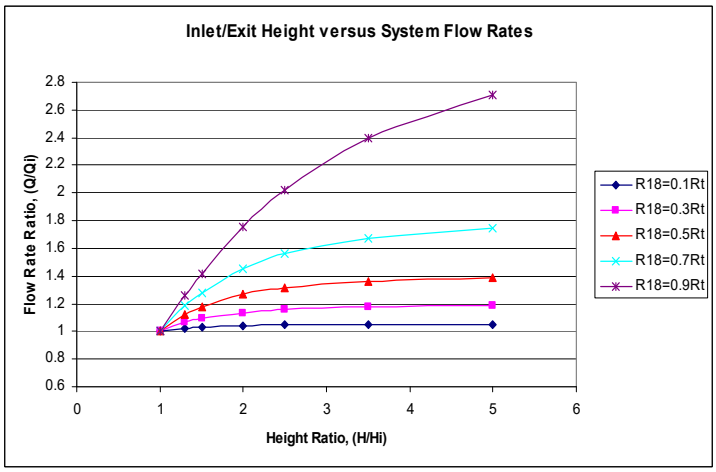

Figure 5 Inlet/Exit Height versus System Flow Rates

-- Effect of System Depth

Figure 6 will be used to examine the effect of the shelf depth on the system flow rate. The analysis is based on the following assumptions

1) All flow resistance from R1 through R8 of the baseline configuration are known
2) Except the depth, all other dimensions of the system remain unchanged
3) Flow resistance of other sections or parts of the system are unchanged

From Equation (1), one obtains the following relationship for the card cage plus with 2 EMI plates

$$R5 / (R5)bl = [(Ac)bl / Ac]^2 \quad (8)$$

Where Ac (=W*D) is the cross section area of the card cage normal to air flow direction which is identical to the cross section area of the air filter. W and D are the width and the depth of the shelf, respectively.

Equation (8) is further reduced to

$$R5 / (R5)bl = [(Dbl)^2 /D^2)] \quad (9)$$

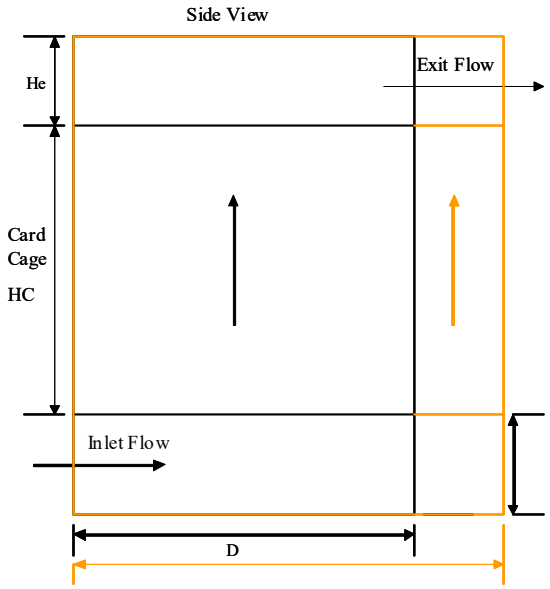

Figure 6 Sketch of System with Various Depths

Similarly to the above calculating procedures, the next step is to compute the new system flow resistance and the new system flow rate. The effects of the system depth on the flow resistance and the flow rate are given in Figures 7 and 8, respectively.

It should be noted all results in Figures 4,5,7 and 8 are normalized to the values of the baseline. In other words, the starting point of the family curves in the above figures represents the baseline values.

For convenience to users, the new family of curves is developed based on R1278 and R45. The R1278 represents the combined flow resistance of the entire section of the inlet and the exit. Similarly, the R45 corresponds to the combined flow resistance of the card cage (over printed circuit boards), 2 EMI plates and the air filter. The new family curves are presented in Figure 9 and 10 for the effects due to varying height and depth, respectively.

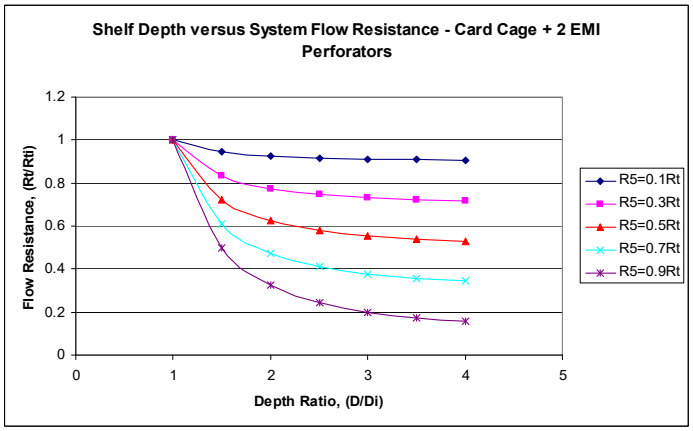

Figure 7 Flow Resistance versus System Depth Ratios

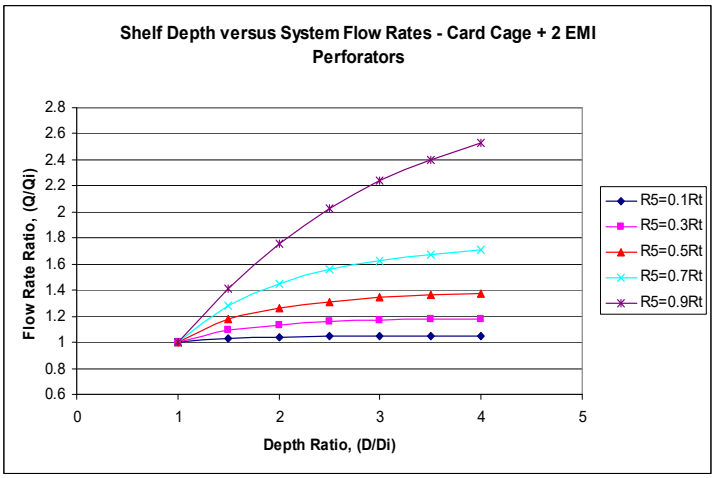

Figure 8 System Flow Rate Ratios over System Depth Ratios

3. Analysis/Design Procedure

The analysis/design optimization procedure can be described as follow:

1) Performing CFD analysis or testing on the initial baseline configuration to obtain the system flow rate,Q0 and all flow resistance (R1 through R8)bl. The obtained results will be the starting point in the above figures. (Figures 4 or 9)

2) Increasing the height of the inlet and/or exit section to a desired value while keeping the system depth unchanged. The new system flow rate, Q1' (=Q1/Q0) (dimensionless) at the adjusted height can be computed from Figure 5 or 9 and this new value will serve as the starting point of Figure 8 or 10

3) Varying the depth to the desired value with the height of the inlet and exit section fixed at the value of Step 2. The system flow rate, Q2' (=Q2/Q1) (dimensionless) for the adjusted depth can be determined from Figure 8 or 10

4) The system final dimensionless flow rate is the product of Q1 and Q2 and the dimensional flow rate is Q0*Q1'*Q2'

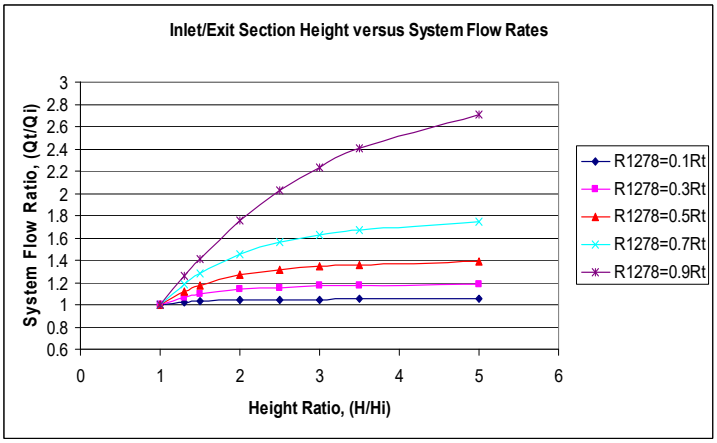

Figure 9 Effect of System Inlet/Exit Height on System Flow Rate

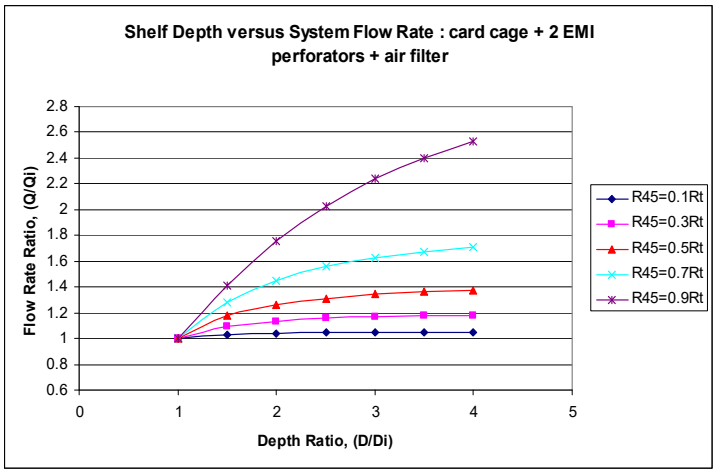

Figure 10 Effect of System Depth on System Flow Rate

It should be noted that the sequence of Steps 2 and 3 is interchangeable. The present analysis is to provide a quick result to evaluate the effects of the parameters of the shelf configuration on the system flow rates. The analysis is based on the assumption of the flow resistance for other sections of the system remain unchanged. The guideline with the dimensionless form is developed for general applications.

The following example will show the calculation procedure about how to utilize the above two figures to obtain the new system flow rate

Example 2:

A 19" telecommunication shelf with 12U height is under consideration. The height of the inlet and exit is 1U. The system includes 14 slots and 12 axial fans. The individual fan power consumption is 24.96 W. The results from the CFD analysis on this baseline configuration indicate that (R18)bl = 0.5447 (Rt)bl and (R45)bl = 0.3 (Rt)bl. Examine the effects on the system flow rate (1) if the inlet and exit height is increased to 1.5U which results in the total height of the shelf of 13U and (2) if the depth is then increased to D/Di = 1.5

(1) **For H/Hi = 1.5 and R18 = 0.5447 Rt**

From Figure 5, We have Qnew/Qbaseline = 1.2 The result indicates that the flow rate is increased by 1.2 times over the flow rate at the baseline configuration when the height of the inlet and exit is increased from 1 to 1.5U.

The potential opportunities due to the increased the system flow rates are as follows:

1) Reducing the fan speeds to save the energy consumption and achieve the system energy efficiency by keeping the system flow rate at the baseline configuration

2) Utilizing this increased the flow rate to reduce component temperatures which leads to higher system reliability. In addition, the results also open the opportunity of using the commercial grade components which are less expensive.

To examine how much energy can be saved, one must understand the operation of the fan laws given below

$$Q = \Phi N D^3 \quad (10a))$$

$$P = \lambda \rho N^3 D^5 \quad (10b)$$

$$p = \psi \rho N^2 D^2 \quad (10c)$$

The variables involved in the above equations are fan size D, rotational speed N. gas density ρ, volumetric flow rate Q, pressure p, power P, and the fan efficiency η. Variables Φ, ψ, and λ are the constants for geometrically and dynamically similar operation and are also referred to as the flow coefficient, pressure coefficient, and power coefficient, respectively.

Following the above fan laws with Qnew/Qbaseline = 1.2

Nnew / Nbaseline = (1 / 1.2) = 0.83

Pnew / Pbaseline = $(0.83)^3$ = 57.9%

Total energy saving = 12 x 24.96 x (1 – 0.579) = 126.1 Watts

Total annual energy saving = 365 x 24 x 126.1 / 1000 = 1104.6 KW-Hr

(2) **For D/Di = 1.5 and R45 = 0.3 Rt**

The new configuration under consideration now is that the depth is increased by 50% while keeping H/Hi = 1.5.

From Figure 8,. We have Q'new/Qnew = 1.1

Q'new / Qbaseline = (Q'new / Qnew) x (Qnew/Qbaseline) = 1.1 x 1.2 = 1.32

N'new / Nbaseline = (1/1.32) = 0.758

P'new / Pbaseline = $(0.758)^3$ = 0.435

Total system energy saving = 12 x 24.96 x (1-0.435) = 169.2 Watts

Total annual energy saving = 365 x 24 x 169.2 / 1000 = 1482.2 KW-Hr

4. Accuracy

It is always not only necessary but also of interest to examine the accuracy of the approximate solutions by comparing with the exact solutions obtained either through analytical or numerical methods. The above family of curves generated is based on the relationship between the pressure drop and the flow resistance as described by Equation (1). The goal of the present analysis is to provide quick solutions to examine the effects of shelf height and/or the shelf depth on the system flow rates so that the system can be optimized to achieve the energy efficiency.

-- Case 1 : R1278 = 0.596 Rt

The height of the inlet and the exit for the system under consideration is 1U for the baseline configuration. The system has 10 fans and the power assumption of each fan is10.56W. The detailed results from the CFD analysis are available for the baseline configuration. Among them, the flow resistance for the inlet/exit section (R1278) is determined to be 0.596 Rt. The additional CFD analyses are also performed for the cases with 2U and 3U inlet/exit heights. The system flow rates and pressure drop computed by CFD analysis for all three configurations are given in Table 1.

Table 1 CFD - System Flow Rate and Pressure Drop

	System Air Flow Rate (CFM)	System Pressure Drop (Pa)	CFM Ratio Over 1U Baseline
Configuration – 1U Inlet/Exit (Baseline)	287.2	163.1	1.0
Configuration – 2U Inlet/Exit	387.5	145.2	1.349
Configuration – 3U Inlet/Exit	429.5	136.9	1.495

Following the calculation procedure described previously, an additional curve for R1278=0.596Rt is added to Figure 10 and the new charts are presented in Figure 11. The reason of creating the new curve for R1278 = 0.596 Rt is to get an accurate result from the charts. For practical applications, the predicted results can be obtained by the interpolation between Curves for R1278 = 0.5 Rt and R1278 = 0.7 Rt from Figure 10.

The graphical flow rate ratios over the height ratios from the above figure are given in Table 2. Table 2 also includes the CFD results which are obtained from Table 1. As can be seen from this table, an excellent agreement is found between the graphical and CFD results.

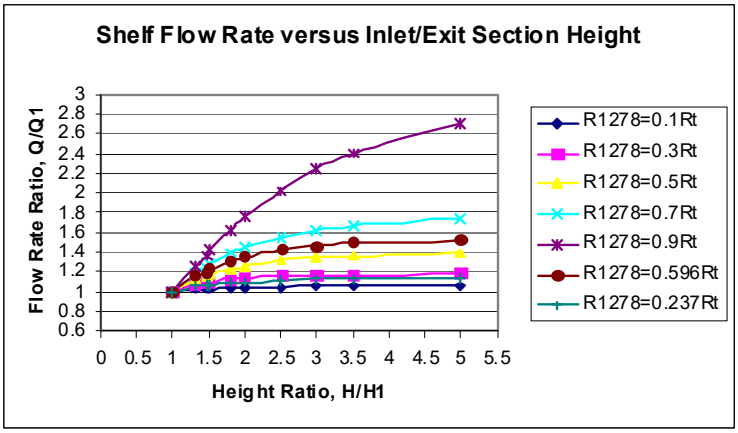

Figure 11 Inlet/Exit Section Height versus System Flow Rate

Table 2 Comparison between CFD and Graphical Results

Height Ratio	Graphical Flow Rate Ratio	CFD Flow Rate Ratio	%Difference
1 (1U)	1.0	1.0	0.00
2 (2U)	1.345	1.349	-0.3
3 (3U)	1.458	1.495	-2.47

-- Case 2 : R1278 = 0.237 Rt

Another case with R1278 = 0.237 Rt was analyzed. Similar to Case 1, an additional curve for R1278 = 0.237 Rt is added to Figure 12 in order to get an accurate result. The graphical results compare very well with the CFD data as presented in Table 3.

Table 3 Comparison between CFD and Graphical Results

Height Ratio	CFD Results	Graphical Flow Rate Ratio	CFD Flow Rate Ratio	%Difference
1 (1.4U)	410 CFM	1.0	1.0	0.00
1.47 (2U)	434.5 CFM	1.067	1.060	0.66
1.79 (2.5U)	440.9 CFM	1.093	1.075	1.67

-- Case 3 : R5 = 0.44 Rt

This case is to study the effect of the shelf depth on the system flow rate. As before, an additional curve for R5 = 0.44 Rt is added to the charts in Figure 8 and the charts are shown in Figure 12. The comparison between the CFD and graphical results are presented in Table 4 and Figure 16. Again, it should be noted the graphical results can directly be obtained by interpolation between Curves for R5 = 0.3 Rt and R5 = 0.5 Rt.

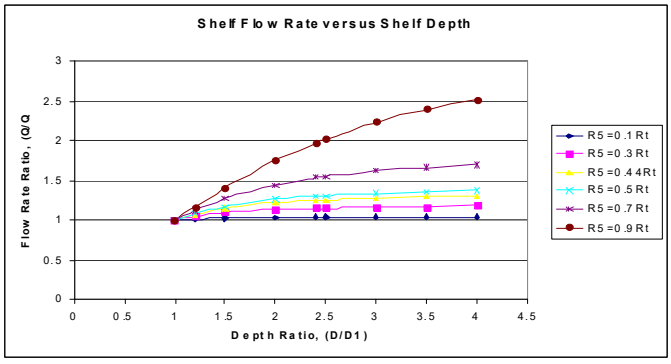

Figure 12 System Flow Ratios versus Shelf Depth Ratios

Table 4 Comparison between CFD and Graphical Results

Height Ratio	CFD Results	Graphical Flow Rate Ratio	CFD Flow Rate Ratio	%Difference
1 (10”)	547.1 CFM	1.0	1.0	0.00
1.2 (12”)	598.1 CFM	1.075	1.09	-1.65
1.5 (15”)	623.8 CFM	1.150	1.140	0.88
2.0 (20”)	640.0 CFM	1.222	1.170	4.44
2.4 (24”)	644.4 CFM	1.254	1.178	6.45

5. Conclusion

A simple but effective method based on the flow network resistance model is developed for the system flow analysis. Though the method can be used to computer the system flow, however this study is focusing at examining the effects of the height and/or depth of the telecommunication rack on the system flow rates. Several sets of the family curves as given in Figuares 5,8,9 and 10 are made to facilitate the analysis and design for practical applications.

The design optimization procedure is presented and the examples with step-by-step illustrations are also provided. In addition, the potential opportunities due to the increased the system flow rates such as reducing energy consumption or increasing the system reliability are discussed.

The comparison between the graphical results generated from the family curves and CFD solutions is made for three cases. The excellent agreement is found in all cases under consideration that further valdiates usefulness of this method.

The current practice in industry is to rerun the CFD analysis each time after the system configuration is changed and the processes involved are time consuming.. It is commonly to investigate a dozen of system configurations in the initial phase of design, especially in the conceptual design phase. With the aids of Figures 5,8,9, and 10, the redesign process only take minutes instead of hours by CFD analysis. It is concluded that the present method which is simple, fast and effective is a very valueable tool in the analysis and design of the telecommunication rack.

References

[1] Blevins, R. D., Applied Fluid Dynamics Handbook, Van Nostrand Reinhold, New York, 1984

[2] Yeh, L.T., and Chu, R. C., Thermal Management of Microelectronic Equipment: Heat Transfer Theory, Analysis Methods and Design Practices, ASME Press, New York, NY, 2002

[3] Yeh, L.T., and Chu, R. C., Thermal Management of Telecommunications Equipment ASME Press, New York, NY 2013